

(1965).

²⁴D. C. Gazis, R. A. Toupin, and R. F. Wallis, *Bull. Am. Phys. Soc.* **8**, 193 (1963).

²⁵R. F. Wallis and D. C. Gazis, in *Lattice Dynamics*, edited by R. F. Wallis (Pergamon, New York, 1965), p. 537.

²⁶A. A. Maradudin and J. Melngailis, *Phys. Rev.* **133**, A1188 (1964).

²⁷D. Schroerer, *Phys. Letters* **21**, 123 (1966).

²⁸D. J. Erickson, L. D. Roberts, T. O. Thomson, and J. W. Burton, *Bull. Am. Phys. Soc.* **15**, 180 (1970).

²⁹F. G. Karioris, J. J. Woyci, and R. R. Buckrey, in *Advances in X-Ray Analysis*, edited by J. B. Newkirk and G. R. Mallett (Plenum, New York, 1967), Vol. 10, p. 250.

³⁰M. H. Rice, R. G. McQueen, and J. M. Walsh, in *Solid State Physics*, edited by F. Seitz and D. Turnbull (Academic, New York, 1958), Vol. 6, p. 1.

³¹S. W. Marshall, Ph. D. thesis, Tulane University, 1965 (unpublished).

³²A. Rothwarf, *Phys. Letters* **30A**, 55 (1969).

PHYSICAL REVIEW B

VOLUME 2, NUMBER 5

1 SEPTEMBER 1970

Electron-Nuclear Double Resonance of Mn^{2+} in KMgF_3 and K_2MgF_4

A. H. M. Schrama and P. I. J. Wouters

Natuurkundig Laboratorium der Universiteit van Amsterdam, The Netherlands*

and

H. W. de Wijn†

Bell Telephone Laboratories, Murray Hill, New Jersey 07974

(Received 23 December 1969)

The ENDOR spectra of $^{55}\text{Mn}^{2+}$ in KMgF_3 and K_2MgF_4 have been measured at 4.2°K. Where- as the spectrum in KMgF_3 could be analyzed in terms of a spin Hamiltonian of cubic symme- try, the spectrum in K_2MgF_4 shows axial anisotropy and appropriate axial terms had to be added. The principal results are for KMgF_3 , $A/hc = (-91.347 \pm 0.007) \times 10^{-4} \text{ cm}^{-1}$; and, for K_2MgF_4 , $D/hc = (+108 \pm 5) \times 10^{-4} \text{ cm}^{-1}$, $A/hc = (-90.809 \pm 0.018) \times 10^{-4} \text{ cm}^{-1}$, $B/hc = (-90.676 \pm 0.014) \times 10^{-4} \text{ cm}^{-1}$, and $Q'/h = 3e^2qQ/40h = (+0.19 \pm 0.04) \text{ MHz}$. A comparison with other compounds indicates that the anisotropic part of the hyperfine structure mainly results from a second-order process, linear in the axial component of the crystalline field and linear in the dipolar hyperfine coupling. Finally, the importance of the D term for the anisotropy field in antiferromagnetic K_2MnF_4 is pointed out.

I. EXPERIMENTAL RESULTS

In this paper we report electron-nuclear double resonance (ENDOR) measurements of the $^{55}\text{Mn}^{2+}$ ($S = \frac{5}{2}$, $I = \frac{5}{2}$) d^5 ^6S -state ion in KMgF_3 and K_2MgF_4 . KMgF_3 has the cubic perovskite structure,¹ and the paramagnetic impurity Mn replaces Mg, which is at a site of cubic point symmetry with a sixfold coordination of nearest-neighbor F ions. K_2MgF_4 is a layer compound with tetragonal unit cell closely related to the perovskite structure.² Again Mn is in a sixfold coordination of F ions, but the cubic arrangement is slightly distorted along the crystalline c axis. The electron-spin resonance spectra (ESR) of these compounds have been studied previously.^{3,4}

The data were taken at a temperature of 4.2°K and a microwave frequency of 8.95 GHz with the experimental setup described previously.^{5,6} The microwave power was increased to saturate the

ESR spectrum to about half of the unsaturated intensity ($\gamma^2 H_1^2 T_1 T_2 \approx 1$). The Mn content of the crystals was between 0.1 and 1%. Roughly speak- ing, the ENDOR spectra each consists of six groups of five lines centered at the approximate frequen- cies of 95, 175, 380, 440, 670, and 690 MHz. Be- cause of inhomogeneous broadening of the ESR lines, the ENDOR transitions were observable over several hundred gauss. The ENDOR frequencies were found to vary by a few percent in going from 2900 to 3400 G. The detailed analysis of the spec- tra has been done by means of diagonalization of the spin-Hamiltonian matrix, including all off- diagonal elements, followed by least-squares ad- justment of the spin-Hamiltonian parameters to the measured line frequencies, as described be- fore.⁶ It appears that the six groups of lines are to be assigned to $m_S = -\frac{1}{2}$, $+\frac{1}{2}$, $-\frac{3}{2}$, $+\frac{3}{2}$, $-\frac{5}{2}$, and $+\frac{5}{2}$, respectively.

The ENDOR lines of Mn: KMgF_3 have been fitted

to the cubic spin Hamiltonian

$$\begin{aligned} \mathcal{H} = & g\beta\vec{H} \cdot \vec{S} + A\vec{S} \cdot \vec{I} - g_I\beta_N\vec{H} \cdot \vec{I} \\ & + \frac{1}{6}a[S_x^4 + S_y^4 + S_z^4 - \frac{1}{5}S(S+1)(3S^2 + 3S - 1)] \\ & + U[S_x^3I_x + S_y^3I_y + S_z^3I_z - \frac{1}{5}(3S^2 + 3S - 1)\vec{S} \cdot \vec{I}] , \quad (1) \end{aligned}$$

in which x , y , and z refer to the cubic axes of the crystal. The results are given in Table I.

Whereas in the case of Mn:KMgF₃ the ENDOR lines are only very slightly dependent on the orientation of the crystal because of the a and U terms, in the case of Mn:K₂MgF₄ a pronounced anisotropy has been found, as is shown in Fig. 1 for the $m_S = -\frac{5}{2}$ and $+\frac{5}{2}$ groups. The spin Hamiltonian had to be augmented by a number of axial terms,⁷ reflecting the axial crystalline-field splitting, nuclear quadrupole coupling, and anisotropy in the hyperfine structure:

$$\begin{aligned} \mathcal{H} = & g\beta\vec{H} \cdot \vec{S} + D[S_z^2 - \frac{1}{3}S(S+1)] + AS_zI_z + B(S_xI_x + S_yI_y) - g_I\beta_N\vec{H} \cdot \vec{I} + Q'[I_z^2 - \frac{1}{3}I(I+1)] \\ & + \frac{1}{6}a[S_x^4 + S_y^4 + S_z^4 - \frac{1}{5}S(S+1)(3S^2 + 3S - 1)] \\ & + \frac{1}{180}F[35S_z^4 - 30S(S+1)S_z^2 + 25S_z^2 - 6S(S+1) + 3S^2(S+1)^2] + U[S_x^3I_x + S_y^3I_y + S_z^3I_z - \frac{1}{5}(3S^2 + 3S - 1)\vec{S} \cdot \vec{I}] , \quad (2) \end{aligned}$$

with

$$Q' = 3e^2qQ/4I(2I-1) , \quad (3)$$

and where the z axis coincides with the tetragonal axis of the crystal. The electronic g factor has been taken to be isotropic instead of axial with components g_{\parallel} and g_{\perp} since g factors determined by ENDOR (after all, a nuclear resonance) are not sufficiently accurate to detect any g anisotropy in the case of the S -state ion Mn²⁺. The nine constants in the spin-Hamiltonian equation (2) were fitted to all experimental line frequencies, both with the magnetic field along the c axis and with the field along the a axis. The results are given in Table II.

II. DISCUSSION

In Fig. 2, the relative anisotropy of the hyperfine structure $(A - B)/A$ has been plotted versus the nuclear quadrupole coupling constant Q' for Mn²⁺ substituted in the four compounds for which these data are available, viz., Al₂O₃,⁸ CaWO₄,⁹ La₂Mg₃(NO₃)₁₂ · 24H₂O (two inequivalent Mn sites),¹⁰ and K₂MgF₄. The experimental material is not abundant, but nevertheless it suggests that there exists a linear relationship between the anisotropic hyperfine structure and the nuclear quadrupole coupling. In other words, since the nuclear quadrupole coupling may be considered to be a direct

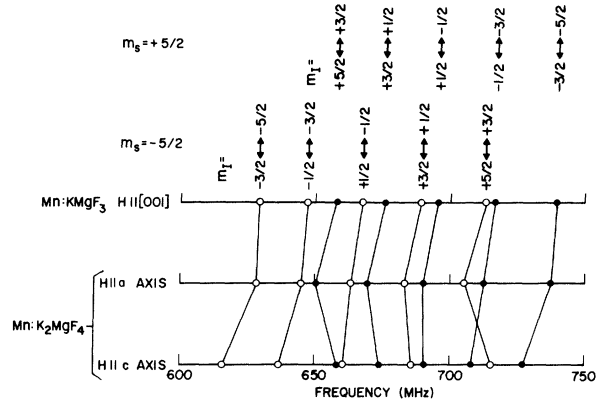


FIG. 1. Positions of ENDOR lines at 3200 G in the $m_S = -\frac{5}{2}$ and $m_S = +\frac{5}{2}$ groups, showing the anisotropy in the case of Mn:K₂MgF₄. Line positions of Mn:KMgF₃ are given for comparison.

experimental measure for the axial component of the crystalline field, the anisotropic part of the hyperfine structure is proportional to the axial crystalline field.

If the ground state of Mn²⁺ were a pure $3d^5 6s$ state, no anisotropy in the hyperfine structure would be expected. However, perturbations of various orders will admix other multiplets of the ground-state configuration $3d^5$, and also multiplets of excited configurations, such as $3d^4 4s$. Interactions which could invoke anisotropy of the hyperfine structure in the presence of axial crystalline fields, i. e., interactions linearly dependent on the nuclear spin I and involving the electronic orbitals, are the orbital hyperfine interaction

$$W_{\text{hf},\text{or}} = 2g_I\beta_N \sum_i (\vec{I}_i \cdot \vec{I} / r_i^3) , \quad (4)$$

and the dipole-dipole hyperfine interaction

TABLE I. Spin-Hamiltonian parameters of ⁵⁵Mn²⁺ in KMgF₃ at 4.2 °K.

g	2.003 ± 0.004
$g_I\beta_N/h$ (10^{-4} MHz/G)	$+ 10.40 \pm 0.14$
A/h (MHz)	$- 273.85 \pm 0.02$
A/hc (10^{-4} cm ⁻¹)	$- 91.347 \pm 0.007$
$ a/hc $ (10^{-4} cm ⁻¹)	< 2
$ U/h $ (MHz)	< 0.03

$$W_{\text{hfs,dd}} = 2g_I\beta\beta_N \sum_i \left(\frac{3(\vec{s}_i \cdot \vec{r}_i)(\vec{I} \cdot \vec{r}_i)}{r_i^5} - \frac{\vec{s}_i \cdot \vec{I}}{r_i^3} \right). \quad (5)$$

Dipole-dipole hyperfine interaction contributes to the anisotropic part of the hyperfine structure

through a second-order process via $3d^4 4s^6 D$ as the intermediate state. The effect is of the order of

$$\frac{\langle 3d^5 {}^6S | W_{\text{hfs,dd}} | 3d^4 4s {}^6D \rangle \langle 3d^4 4s {}^6D | W_{\text{ax}} | 3d^5 {}^6S \rangle}{E(3d^4 4s {}^6D) - E(3d^5 {}^6S)}, \quad (6)$$

where W_{ax} is the axial crystalline-field potential. This mechanism is analogous to the mechanism proposed by Pryce¹¹ for the D term of the spin Hamiltonian, as can be observed by replacing the electron-spin-electron-spin coupling by the dipole-dipole hyperfine interaction. In an order-of-magnitude calculation, we may put, for Mn^{2+} , $W_{\text{hfs,dd}} \approx 0.001 \text{ cm}^{-1}$, $W_{\text{ax}} \approx 1000 \text{ cm}^{-1}$, and for the excitation energy 60000 cm^{-1} .¹² This results in an order of magnitude of 0.6 MHz for the anisotropy in the hyperfine structure, which is consistent with the observed effects. The mechanism described by Eq. (6) might also be effective through other excitations of the type $3d \rightarrow ns$, and through additional excitations of the types $3d \rightarrow nd$ and $3d \rightarrow ng$, excitations which also contribute to the Pryce mechanism for the D term.¹³ Still another mechanism, a third-order process involving the orbital hyperfine structure, is

$$\frac{\langle 3d^5 {}^6S | W_{\text{hfs,or}} | 3d^4 4d {}^6P \rangle \langle 3d^4 4d {}^6P | W_{\text{ax}} | 3d^4 4d {}^6P \rangle \langle 3d^4 4d {}^6P | W_{\text{LS}} | 3d^5 {}^6S \rangle}{[E(3d^4 4d {}^6P) - E(3d^5 {}^6S)]^2}, \quad (7)$$

where W_{LS} is the spin-orbit coupling. Its contribution is, however, smaller by at least an order of magnitude as compared to Eq. (6).

The mechanisms discussed above are *linear* in the axial crystalline field, in agreement with experiment. It is of interest to point out that one cannot construct a contribution to the anisotropic hyperfine structure *quadratic* in the axial field in analogy with the contribution of the D term proposed by Watanabe,¹⁴

$$\frac{\langle {}^6S | W_{\text{LS}} | {}^4P \rangle \langle {}^4P | W_{\text{ax}} | {}^4D \rangle \langle {}^4D | W_{\text{ax}} | {}^4P \rangle \langle {}^4P | W_{\text{LS}} | {}^6S \rangle}{[E({}^4P) - E({}^6S)]^2 [E({}^4D) - E({}^6S)]}, \quad (8)$$

where all excitations are within the $3d^5$ configuration. If we replace one of the spin-orbit matrix elements in Eq. (8) by the corresponding element of the orbital hyperfine structure, the interaction vanishes because the latter has zero matrix elements between quartets and sextets. By the same argument, the analogies (again replacing one of the spin-orbit matrix elements by the orbital hyperfine structure) of the D -term mechanisms of Blume and Orbach¹⁵ and of Orbach, Das, and Sharma¹³ are zero. Further, replacement of a spin-orbit matrix element by the dipolar hyperfine coupling does not contribute by virtue of time-reversal symmetry. In summary, anisotropic hyperfine structure results mainly from second-order processes involving first powers of axial crystalline field and dipolar hyperfine coupling, Eq. (6), whereas the D term of the spin Hamiltonian is at least a quadratic function of the axial field.

The axial symmetry of the Mn site is also reflected in the presence of nuclear quadrupole coupling. Using¹⁶

$$Q({}^{55}\text{Mn}) = +0.35 \times 10^{-24} \text{ cm}^2,$$

and the antishielding factor¹⁷ $\gamma_\infty({}^{55}\text{Mn}) = -11.4$, we arrive at an "experimental" field gradient

$$q_p = (e^2 q Q) / e^2 (1 - \gamma_\infty) Q = +0.013 \times 10^{24} \text{ cm}^{-3}.$$

This value is to be compared with the electric field gradient calculated from the point-charge model (K_2MnF_4 is almost completely ionic, so that covalency effects are expected to be small),

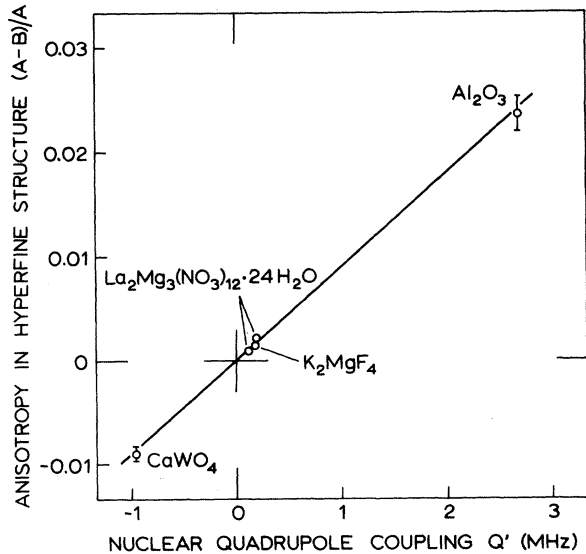


FIG. 2. Anisotropy in the hyperfine structure $(A-B)/A$ of Mn^{2+} ions in various compounds versus the nuclear quadrupole coupling $Q' = 3e^2 q Q / 40$.

$$q_p = -\sum_i Z_i [(3 \cos^2 \theta_i - 1)/R_i^3], \quad (9)$$

where θ_i is the angle of the radius vector \vec{R}_i with respect to the tetragonal axis and Z_i is the number of unit charges on the ion. The interatomic distances in the unit cell of K_2MgF_4 have not been studied, but, to a first approximation, the sixfold F coordination of Mn^{2+} ion at a Mg site is cubic, so that the contributions from the six first F neighbors cancel. Both the K^+ and the other F^- ions contribute negatively to q_p by a total of $-0.024 \times 10^{24} \text{ cm}^{-3}$ and $-0.094 \times 10^{24} \text{ cm}^{-3}$, respectively, but their total contribution is eclipsed by the Mg^{2+} ions, which contribute by $+0.136 \times 10^{24} \text{ cm}^{-3}$, originating mainly from the Mg^{2+} ions in the layer.¹⁸ For a cubic nearest-neighbor F coordination we therefore have $q_p = +0.018 \times 10^{24} \text{ cm}^{-3}$, which has both the correct sign and correct magnitude. This value is, however, quite sensitive to distortion of the cubic nearest-neighbor F coordination, and in fact a 0.4% elongation along the crystalline tetragonal axis makes the point charge q_p to coincide with the experimental value. For comparison, it is noted that in the magnetically undiluted K_2MnF_4 , for which the unit cell has been studied by neutron diffraction,¹⁹ an elongation of the F coordination by $(1.3 \pm 0.7)\%$ has been found.

We finally point out the importance of the axial crystalline-field splitting D in any detailed discussion of the antiferromagnetic state involving the single-ion anisotropy, such as the determination of zero-point spin reduction from the spin-flop field. In the ordered antiferromagnet K_2MnF_4 , the anisotropy field H_A is known to be mainly dipolar in origin. With the magnetic unit cell constants¹⁹ $a = 5.871 \text{ \AA}$ and $c = 13.242 \text{ \AA}$, lattice summation¹⁸ over $(3 \cos^2 \theta - 1)/r^3$ yields $H_A = 2572 \text{ Oe}$, if no spin reduction is present. By equating the decrease of the magnetization energy and the increase of the anisotropy energy

$$\frac{1}{2}(\chi_{\perp} - \chi_{\parallel})H_{TF}^2 = MH_A, \quad (10)$$

where H_{TF} is the threshold field and M is the sub-

TABLE II. Spin-Hamiltonian parameters of $^{55}\text{Mn}^{2+}$ in $K_2\text{MgF}_4$ at 4.2°K.

$g = g_{\parallel} = g_{\perp}$	2.004 ± 0.005
$g_I \beta_N / h$ (10^{-4} MHz/G)	$+ 10.31 \pm 0.16$
D/hc (10^{-4} cm $^{-1}$)	$+108 \pm 5$
A/h (MHz)	-272.24 ± 0.05
A/hc (10^{-4} cm $^{-1}$)	-90.809 ± 0.018
B/h (MHz)	-271.84 ± 0.04
B/hc (10^{-4} cm $^{-1}$)	-90.676 ± 0.014
Q'/h (MHz)	$+ 0.19 \pm 0.04$
$ a/hc $ (10^{-4} cm $^{-1}$)	< 5
$ U/h $ (MHz)	< 0.06
F/h (10^{-4} cm $^{-1}$)	$+ 30 \pm 20$

lattice magnetization, Breed²⁰ has shown that good agreement with experiment is obtained if both M and H_A are reduced by 7.88%, that is, the value of the spin reduction predicted by spin-wave theory for a quadratic lattice of spins $S = \frac{5}{2}$ without anisotropy. No allowance was made, however, for the crystalline contribution to the anisotropy, which, as the dipolar part, has a $(3 \cos^2 \theta - 1)$ angular dependence and therefore is additive:

$$H_A = H_{A, \text{dd}} + (D/g\beta)(1 - 2S). \quad (11)$$

Taking the value of D derived from the present experiments on $Mn:K_2MgF_4$, we arrive at a crystalline contribution to the anisotropy field of -460 G , which is 18% of the dipole-dipole part. If the parameter D in K_2MnF_4 were the same as in K_2MgF_4 , Breed's value for the threshold field would imply an unreduced expectation value of the spin. On the other hand, the D term of $Mn:K_2ZnF_4$ has been measured²¹ to be $D = 35.4 \times 10^{-4} \text{ cm}^{-1}$, about three times smaller. By comparing the lattice parameters of K_2MnF_4 with those of K_2MgF_4 and K_2ZnF_4 , one expects D for K_2MnF_4 to be closer to the value of K_2ZnF_4 , which would indicate the spin deviation to be roughly 70% of the spin-wave value. It is, however, clear that definite conclusions regarding the spin reduction in antiferromagnetic K_2MnF_4 cannot be drawn from the observed threshold field.

*Work performed in Amsterdam supported by the Foundations F. O. M. and Z. W. O.

[†]On leave of absence from the Natuurkundig Laboratorium der Universiteit van Amsterdam, The Netherlands.

¹R. W. G. Wyckoff, *Crystal Structures*, 2nd ed. (Interscience, New York, 1964), Vol. 2, p. 392

²Reference 1, Vol. 3, pp. 68, 69.

³S. Ogawa, J. Phys. Soc. Japan **15**, 1475 (1960).

⁴T. P. P. Hall, W. Hayes, and F. I. B. Williams, Proc. Phys. Soc. (London) **78**, 883 (1961).

⁵Y. H. Eskes and H. W. de Wijn, Phys. Letters **25A**, 553 (1967).

⁶H. W. de Wijn and A. H. M. Schrama, J. Chem. Phys. **49**, 2971 (1968).

⁷S. Geschwind, Phys. Rev. **121**, 363 (1961).

⁸J. J. Krebs, J. Lambe, and N. Laurance, Phys. Rev. **141**, 425 (1966).

⁹W. B. Mims, G. E. Devlin, S. Geschwind, and V. Jaccarino, Phys. Letters **24A**, 481 (1967).

¹⁰R. de Beer and D. van Ormondt, Phys. Letters **27A**, 475 (1968).

¹¹M. H. L. Pryce, Phys. Rev. **80**, 1107 (1950).

¹²C. E. Moore, Natl. Bur. Std. (U. S.) Circ. No. 467 (1949).

¹³R. R. Sharma, T. P. Das, and R. Orbach, Phys. ,

Rev. **149**, 257 (1966); **171**, 378 (1968).

¹⁴H. Watanabe, Progr. Theoret. Phys. (Kyoto) **18**, 405 (1957).

¹⁵M. Blume and R. Orbach, Phys. Rev. **127**, 1587 (1962).

¹⁶H. Walther, Z. Physik **170**, 507 (1962).

¹⁷R. M. Sternheimer, Phys. Rev. **146**, 140 (1966).

¹⁸The lattice summations over $(3 \cos^2 \theta - 1)/r^3$ have

been carried out with a computer program employing the Ewald-Kornfeld method.

¹⁹B. O. Loopstra, B. van Laar, and D. J. Breed, Phys. Letters **26A**, 526 (1968); **27A**, 188 (1968).

²⁰D. J. Breed, Physica **37**, 35 (1967).

²¹M. Rubenstein and V. J. Folen, Phys. Letters **28A**, 108 (1968); V. J. Folen, J. Appl. Phys. **40**, 1370 (1969).

PHYSICAL REVIEW B

VOLUME 2, NUMBER 5

1 SEPTEMBER 1970

Iron-Arsenic Associates in ZnSe^\dagger

R. K. Watts

Texas Instruments Incorporated, Dallas, Texas

(Received 13 April 1970)

Electron paramagnetic resonance of Fe^{3+} in the strong trigonal field of a nearest-neighbor substitutional arsenic in ZnSe is reported. Superhyperfine structure is observed from the four nearest neighbors — one arsenic and three seleniums. The parameters appearing in an effective spin Hamiltonian with $S = \frac{1}{2}$ are $g_{\parallel}^e = 2.0238$, $g_{\perp}^e = 6.168$, $A(\text{Fe}^{57}) = 6.2 \times 10^{-4} \text{ cm}^{-1}$, $B(\text{Fe}^{57}) = 16.8 \times 10^{-4} \text{ cm}^{-1}$, $K_{\parallel}(\text{As}^{75}) = 8.71 \times 10^{-4} \text{ cm}^{-1}$, and $K_{\perp}(\text{As}^{75}) = 16.20 \times 10^{-4} \text{ cm}^{-1}$.

I. INTRODUCTION

Impurity associates are rather common in the II-VI compounds.^{1,2} Fe^{3+} has been shown to associate in them with copper, silver, or lithium at a next-nearest-neighbor lattice site, the magnetic properties being those of $(3d)^5 6S$ in a field of C_s symmetry.² This paper reports magnetic resonance of Fe^{3+} in the strong trigonal field produced by a nearest-neighbor arsenic associate in ZnSe .

II. MEASUREMENTS

ZnSe was compounded by allowing elemental zinc to react with H_2Se gas. Small amounts of arsenic and iron were added, and single crystals were grown from the melt in a sealed ampoule by a gradient-freeze technique.³ Resonances were observed at 1.3 K with a superheterodyne spectrometer operating at 9 GHz. The crystals were mounted on the end of a quartz light pipe which extended along the axis of the right circular cylindrical cavity. The crystals could be irradiated through the light pipe with light from a 1.5-kW mercury-arc lamp and monochromator. The magnetic field was rotated in a $\{110\}$ crystallographic plane.

In all samples, a weak signal consisting of four lines and smaller satellites with g factor 2 for the magnetic field along a $\langle 111 \rangle$ axis and 6 for the field perpendicular to the axis was observed. See Figs. 1 and 2. The signal is much weaker than that due to unassociated arsenic⁴ and is observed also in samples not intentionally doped with iron. Iron is a common contaminant in all II-VI compounds. Iron doping increases the strength of the signal.

Doping with iron isotopically enriched to 98% Fe^{57} with nuclear spin $\frac{1}{2}$ causes a doubling of the number of spectral lines, as shown in Figs. 3 and 4. In this manner Fe^{3+} is identified as the paramagnetic ion. A strong axial electric field is known to produce the observed g factors. The four equally intense lines of the spectra are interpreted to arise from the hyperfine interaction with an As ion on the symmetry axis; in fact, this ion defines this axis. The angular dependence of the spectrum is described by the effective spin Hamiltonian⁵

$$\begin{aligned} \mathcal{H}^e = & g_{\parallel}^e \beta H_z S_z + g_{\perp}^e \beta (H_x S_x + H_y S_y) + A(\text{Fe}^{57}) I_z \\ & \times (\text{Fe}) S_z + B(\text{Fe}^{57}) [I_x(\text{Fe}) S_x + I_y(\text{Fe}) S_y] \\ & + K_{\parallel}(\text{As}^{75}) I_z(\text{As}) S_z + K_{\perp}(\text{As}^{75}) [I_x(\text{As}) S_x \\ & + I_y(\text{As}) S_y] + \sum_{i=1}^3 \vec{S} \cdot \vec{K}(\text{Se}^{77}) \cdot \vec{I}(\text{Se}), \end{aligned} \quad (1)$$

where

$$g_{\parallel}^e = 2.0238 \pm 0.0005,$$

$$A(\text{Fe}^{57}) = (6.2 \pm 0.2) \times 10^{-4} \text{ cm}^{-1},$$

$$g_{\perp}^e = 6.168 \pm 0.002,$$

$$B(\text{Fe}^{57}) = (16.8 \pm 0.7) \times 10^{-4} \text{ cm}^{-1},$$

$$K_{\parallel}(\text{As}^{75}) = (8.71 \pm 0.15) \times 10^{-4} \text{ cm}^{-1}, \quad S = \frac{1}{2}$$

$$K_{\perp}(\text{As}^{75}) = (16.20 \pm 0.68) \times 10^{-4} \text{ cm}^{-1}, \quad \hat{z} \parallel \langle 111 \rangle.$$

The small satellite lines seen in the figures are interpreted as a superhyperfine spectrum from three selenium nuclei. When the magnetic field is along the $\langle 111 \rangle$ symmetry axis these three nuclei are magnetically equivalent. In this case two satellites about each main line with intensity 0.11 rela-